Nanoscale

COMMUNICATION

View Article Online
View Journal | View Issue



Cite this: *Nanoscale*, 2016, **8**, 3232

Received 10th December 2015,
Accepted 8th January 2016

DOI: 10.1039/c5nr08784h

www.rsc.org/nanoscale

# Dry shear aligning: a simple and versatile method to smooth and align the surfaces of carbon nanotube thin films†

D. D. Tune,*[a,b] B. W. Stolz,[a] M. Pfohl[a] and B. S. Flavel*[a]

**We show that the application of lateral shear force on a randomly oriented thin film of carbon nanotubes, in the dry state, causes significant reordering of the nanotubes at the film surface. This new technique of dry shear aligning is applicable to carbon nanotube thin films produced by many of the established methods.**

The alignment of carbon nanotubes in thin films parallel to a surface is a topic of widespread research interest in the nanotube community. This is because, when carbon nanotubes are present as a randomly ordered bulk material, some of the often-touted electronic and optical properties of the individual nanotubes are suppressed, which confounds their full exploitation in a variety of devices and applications. We show here a new method of smoothing and aligning carbon nanotube thin films that is both inherently scalable and exceedingly simple. Depending on the type and purity of the nanotubes, the technique can also provide excellent surface alignment of the nanotubes in a dense and close packed array. A number of techniques of producing smooth and aligned carbon nanotube thin films over large areas have been reported with varying degrees of complexity, difficulty, and scalability, as well as resultant degree of nanotube alignment. These include the collapse of vertically aligned arrays[1–6] or exfoliation of CVD grown forests,[7,8] horizontal CVD growth,[9] use of Langmuir-Blodgett[10] or Langmuir-Schaeffer[11] deposition, solution shearing from superacids[12,13] or polyelectrolyte salt solutions[14] at liquid crystal concentrations of nanotubes, shear alignment in a liquid film followed by filtration,[15] evaporation-driven self-assembly of sidewall-functionalised[16] or surfactant-stabilised suspensions,[17,18] and floating evaporative self-assembly.[19] Whilst successful, many of these techniques require very specific preparation and some have limited applicability beyond the laboratory environment. In contrast, this Communication reports a simple method of smoothing and aligning the surfaces of carbon nanotube thin films on substrates by applying lateral shear force to the films in the dry state. The new technique is fundamentally different to other methods such as the collapse or 'pushing over' of dense and ordered arrays[1–6] which are already aligned in the vertical direction and are either reoriented by up to 90° to become horizontally aligned or are bent so that part of the length of each nanotube is more or less parallel to the surface. It is also different to the alignment of nanoparticles by drag forces in a thin liquid film followed by filtration,[15] or of nanotube liquid crystals.[12–14]

As illustrated in Fig. 1, the process of dry shear aligning (DSA) is straightforward; involving the application of compressive force between an aligner and a substrate holding a nanotube film and then shearing of the aligner relative to the substrate. As exemplified in the SEM images shown in Fig. 2, the effects on nanotube film morphology can be dramatic. Before DSA, the films are composed of dense mats of randomly oriented and interwoven nanotube bundles, with bundle diameters and film roughness varying depending on the technique used to form the film. After DSA, the nanotubes on the surface of the films are uniformly oriented in the direction of shear and have been densified. So far, in our labs, we have applied the DSA technique to small and large diameter single walled nanotubes, double walled nanotubes and multiwalled nano-

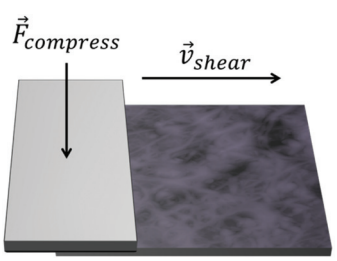


**Fig. 1** Schematic of the dry shear aligning process.

[a]*Institute of Nanotechnology, Karlsruhe Institute of Technology, 76021 Karlsruhe, Germany. E-mail: daniel.tune@kit.edu, benjamin.flavel@kit.edu*
[b]*Centre for Nanoscale Science and Technology, Flinders University, Adelaide 5042, Australia*

†Electronic supplementary information (ESI) available: Detailed experimental methods, table of nanotube details, absorption spectra, further SEM data, plots of sheet resistance, DC to optical conductivity, and 2D order parameter as a function of transmittance. See DOI: 10.1039/c5nr08784h

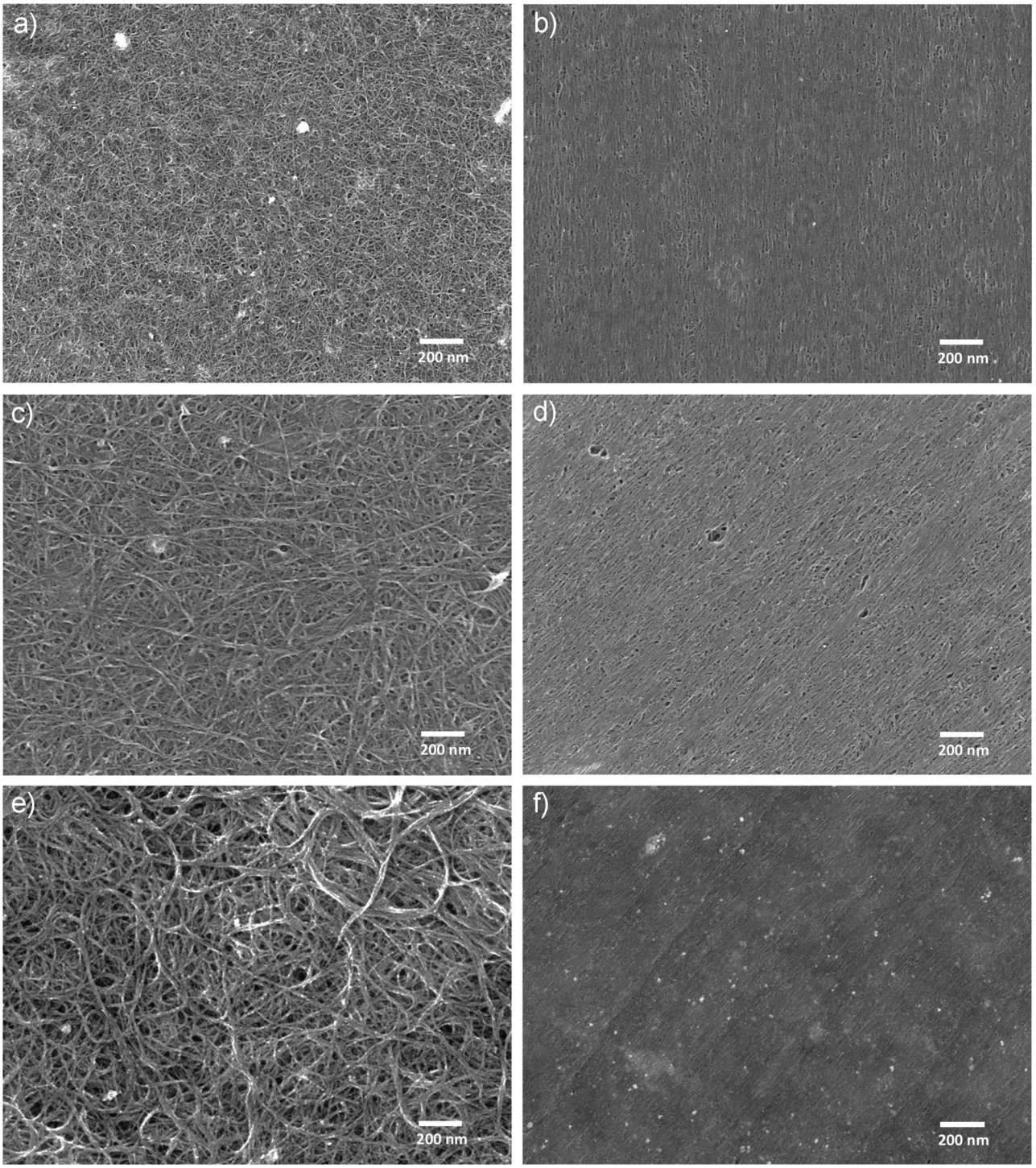


**Fig. 2** SEM images of (a, c, e) as-prepared nanotube films and (b, d, f) the same films after dry shear aligning, where the film in (a) and (b) was produced by slide casting of HiPco nanotubes (SuperPureTubes, NanoIntegris) dissolved in sodium polyelectrolyte solution and had an order parameter after DSA of $S_{2D}$ = 0.41, the film in (c) and (d) was produced by slide casting of gel sorted, small diameter metallic nanotubes made from raw HiPco material (NanoIntegris) and dissolved in sodium polyelectrolyte solution and had an order parameter after DSA of $S_{2D}$ = 0.28, and the film in (e) and (f) was produced by vacuum filtration onto a mixed cellulose ester membrane (HAWP, Merck Millipore) of raw HiPco material suspended in 1 wt% SDS solution and had an order parameter after DSA of $S_{2D}$ = 0.22. In all cases DSA was conducted on the films mounted on glass slides. Absorption spectra of the three kinds of nanotube film are shown in Fig. S1.†

tubes stabilised with surfactants, as well as those dissolved in chlorosulphonic acid or sodium polyelectrolyte solutions at concentrations below that required for liquid crystal ordering (if they were at liquid crystal concentration then the film formation process would already align the nanotubes, negating the need for DSA). The resultant level of order of the films follows the trend SW (small) > SW (large) > DW ≫ MW (Fig. S2†). We have observed no difference in the response of semiconducting, metallic or mixed nanotubes although the more pure and free of catalyst particulates and other contaminants the starting material is, the cleaner the final film is. This can be readily seen in Fig. 2(f) where many bright spots of high secondary electron emission are observed, corresponding to metal catalyst particles in the raw nanotube starting material, as well as some regions of blurriness which may correspond to amorphous carbon in the starting material, or perhaps to some residual surfactant. Also seen in Fig. 2(f) are some shallow striations due to the aligner surface (Teflon in this case) not being atomically flat. Better flattening and alignment is observed with higher purity material, whereas extensive damage occurs to the films when particulates are present during shearing (Fig. S3†). DSA can be applied to films created by vacuum filtration from aqueous or non-aqueous suspensions, or shearing/slide casting from isotropic solutions, with varying effects depending on the technique. In the case of vacuum filtration (Fig. S4†), the DSA technique can be applied directly on the film after it has been transferred to a surface (Fig. S4(e–h)†), or on the filtration membrane before transfer (Fig. S4(i–l)†). Or, DSA could be applied before transfer to flatten/align one side of the film and provide an improved junction with the substrate, then after transfer to flatten and align the other side to provide a better junction with any additional material layers in the respective device. Comparing DSA of films made by vacuum filtration of single, double and multiwalled nanotubes (Fig. S4, S5 and S6,† respectively) it is clear that the degree of reorganisation of the nanotubes is heavily dependent on their type and purity. The smaller the diameter of the nanotubes, the easier they are to rearrange and hence the better the flattening and alignment, with the best results obtained from material such as high purity, gel-sorted (6,5) nanotubes[20,21] (Fig. S7†). For the aligner, we use Teflon for films still attached to the filtration membrane, although polycarbonate, ceramic, glass and steel all yield positive results, and latex for films on glass or silicon, though nitrile and rubber are also effective.

Clearly, DSA is inherently scalable to nanotube films of arbitrary size and dimension without complication of the equipment setup since the essential elements are that pressure is applied to an aligner that is in contact with, and moving in relation to, a surface holding a nanotube thin film. In principle this could be applied in continuous roll-to-roll production processes. These characteristics are in stark contrast to some previous alternatives which could only be applied in batch production and which may require expensive tooling and/or add significantly to manufacturing complexity.[3–6,9–11,15] DSA does not require any specific preparation of the nanotubes over and above that required to form the film by a chosen method. Importantly, and in contrast to other potentially industrial-scale techniques such as the collapse or drawing of CVD grown forests, this means that DSA can be applied to the whole range of nanotubes from raw mixtures of type and chirality through to very highly purified, chirality sorted material.

In addition to the long range ordering apparent in Fig. 2, the other main effect of the DSA technique is to significantly reduce the film roughness. Fig. 3(a) and 3(b) show 3D AFM images of a vacuum filtered nanotube film before and after DSA. In this case the root mean squared roughness decreased substantially from 143 nm to just 3.3 nm, an outstanding improvement, and similar large decreases are observed for all the nanotube films we have studied, regardless of whether or not the nanotubes were aligned. The ability to create such smooth films is particularly advantageous in the context of using nanotube films in application where they are used in conjunction with thin layers of other materials. For example, where the nanotubes are used as electrodes or charge transport layers in organic photovoltaics, LEDs, capacitors, *etc.*, in which the thickness of the material layer on top of the nanotubes could be well below 100 nm. As one would predict, the anisotropy induced by DSA causes the nanotube films to have a different response to polarised light depending on orientation. Fig. 3(c) shows the optical spectrum of the film in Fig. 3(a) and is invariant under polarisation. Polarised optical absorption spectra from the same film (the other half of the filtration membrane) after the application of DSA are shown in Fig. 3(d) and yield a 2D order parameter of 0.16, where the order parameter was calculated as per White and Taylor[22] and where

$$S_{2D} = (A_{\parallel} - A_{\perp})/(A_{\parallel} + 2A_{\perp})$$

This value is somewhat less than might be expected based on the SEM images however it must be noted that the alignment occurs only on the surface of thicker films, leaving the inner regions in their randomly oriented state, and this is particularly true when the films are still bound to the filtration membrane; with a proportion of the material penetrating into the pores and less exposed to shear. A comprehensive study of the effect of DSA on varied thicknesses of vacuum filtered films of large diameter single walled nanotubes was conducted (Fig. S8, S9 and S10†). As well as the usual relationships between sheet resistance, thickness and doping which are well captured in the figure of merit ratio of DC electrical to optical conductivity (Fig. S10(a+c)†),[23] the data show both a small but distinct anisotropy in the conductance (Fig. S10(b+d)†) as well as a clear dependence of the extent of nanotube alignment on the film thickness, with a critical thickness corresponding to a transmittance of around $T_{550}$ = 80% (Fig. S11†), above which the effects of DSA become more pronounced. This suggests that future fine tuning of the film thickness and DSA conditions may allow for the production of films composed only of the aligned surface region.

 

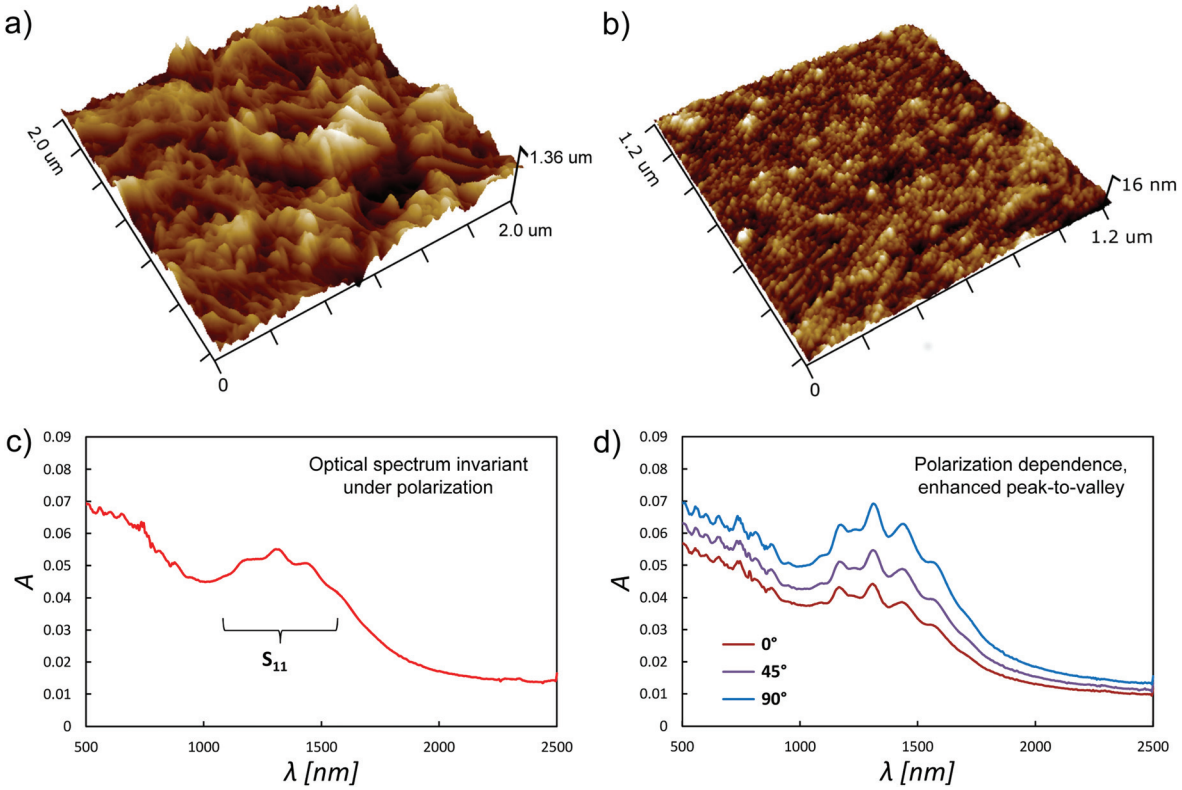


**Fig. 3** (a) and (b) show 3D AFM images of a vacuum filtered nanotube film before and after DSA, respectively, while (c) and (d) show the corresponding polarised optical spectra.

Although the smoothing of the nanotube films is an intuitive process, the mechanism underlying alignment by DSA is not immediately clear. If the nanotubes were subjected to a flowing liquid, as in the case of nanotube fibre formation from chlorosulphonic acid in a faster flowing coagulant,[24] then the alignment could be explained as being due to the well-known effects of drag on the rotation/orientation of an anisotropic particle in a flow. Similarly for cellulose nanocrystals suspended in water, which can be aligned in thin liquid films subjected to doctor blading, as long as the volume concentration of the nanocrystals in the solvent is low enough to allow free movement,[25] and for nematic liquid crystals of carbon nanotubes dissolved by superacids[13] or *via* alkali metal reduction[14] and sheared in a thin liquid film. In such cases the alignment process can be understood in the context of well-known continuum theories modelling liquid crystal behaviour.[26] However, the situation is quite different in the case of a dry material. In determining the mechanism underlying DSA, considerable insight can be found in the work of Börzsönyi *et al.* who studied the shear induced alignment of various elongated particles and developed a numerical model of the experimental observations.[27] The process is shown to be very similar to that occurring in nematic liquid crystals, despite the completely different interparticle interactions involved. In Börzsönyi's model, the fundamental cause of the alignment is a reduction in friction between the material and the shearing plate by up to a third in the aligned state *vs.* the unaligned one. The degree of order scales with the aspect ratio of the individual particles up to 5 : 1 (the upper limit in the experiment). The fact that DSA appears so far to be a surface effect, unlike in the Börzsönyi *et al.* work, in which the degree of order was observed to be the same throughout the material, could be due to, (a) the much higher aspect ratio of the nanotubes (100 : 1 up to >1000 : 1) which, as discussed by Börzsönyi *et al.*, leads to much greater levels of entanglement between neighbours and thus hinders movement of the nanotubes, (b) the extremely low friction that exists between nanotube sidewalls,[28] reducing the penetration depth of the shear force (and perhaps explaining why the order parameter is lower for nanotube films deposited from surfactant-stabilised suspensions *vs.* those deposited from true solutions in superacid, *etc.* – the surface nanotubes are more free to slide past each other without the presence of residual surfactant) and, (c) the fact that in the Börzsönyi *et al.* experiments only one side of the bulk material was subject to a shearing surface whilst the other side was free to move, which is different to the situation in DSA where one side of the film is adhered to a stationary surface. Nevertheless, the model provides a strong foundation for understanding the current work.

In summary, dry shear aligning is a simple post-fabrication treatment that can yield dramatic improvements in film roughness and homogeneity, along with excellent alignment of the

surface nanotubes. Apart from the presentation of a facile and scalable technique to generate outstandingly smooth films from much rougher starting material, the main conclusion of this work is that, perhaps contrary to assumption, carbon nanotube films like the ones used in this work are not fixed structures, but are dynamic and malleable systems containing mobile elements that are capable of significant restructuring and reordering with appropriate mechanical intervention. The observation of realignment of the nanotube bundles reveals the fluidity and plasticity of such films and is a practical insight that may inform future work in the field. Considering the widespread use of thin nanotube films across a broad swath of fundamental and applied nanoscience, we expect that the dry shear aligning technique may be of benefit to many in the nanotube research community.

## Acknowledgements

B. S. Flavel gratefully acknowledges support from the Deutsche Forschungsgemeinschaft's Emmy Noether Programm under grant number FL 834/1-1.

## References

1 B. Chen, G. Zhong, P. Goldberg Oppenheimer, C. Zhang, H. Tornatzky, S. Esconjauregui, S. Hofmann and J. Robertson, *ACS Appl. Mater. Interfaces*, 2015, **7**, 3626–3632.
2 S. Hu, Z. Xia and L. Dai, *Nanoscale*, 2013, **5**, 475–486.
3 M. Cole, P. Hiralal, K. Ying, C. Li, Y. Zhang, K. Teo, A. Ferrari and W. Milne, *J. Nanomater.*, 2012, **2012**, 8.
4 P. D. Bradford, X. Wang, H. Zhao, J.-P. Maria, Q. Jia and Y. T. Zhu, *Compos. Sci. Technol.*, 2010, **70**, 1980–1985.
5 W. Ding, S. Pengcheng, L. Changhong, W. Wei and F. Shoushan, *Nanotechnology*, 2008, **19**, 075609.
6 W. A. deHeer, W. S. Bacsa, A. Châtelain, T. Gerfin, R. Humphrey-Baker, L. Forro and D. Ugarte, *Science*, 1995, **268**, 845–847.
7 L. Zhang, X. Wang, W. Xu, Y. Zhang, Q. Li, P. D. Bradford and Y. Zhu, *Small*, 2015, **11**, 3830–3836.
8 K. Wang, S. Luo, Y. Wu, X. He, F. Zhao, J. Wang, K. Jiang and S. Fan, *Adv. Funct. Mater.*, 2013, **23**, 846–853.
9 L. Ren, C. L. Pint, L. G. Booshehri, W. D. Rice, X. Wang, D. J. Hilton, K. Takeya, I. Kawayama, M. Tonouchi, R. H. Hauge and J. Kono, *Nano Lett.*, 2009, **9**, 2610–2613.
10 G. Giancane, A. Ruland, V. Sgobba, D. Manno, A. Serra, G. M. Farinola, O. H. Omar, D. M. Guldi and L. Valli, *Adv. Funct. Mater.*, 2010, **20**, 2481–2488.
11 Q. Cao, S.-J. Han, G. S. Tulevski, Y. Zhu, D. D. Lu and W. Haensch, *Nat. Nanotechnol.*, 2013, **8**, 180–186.
12 S. Park, G. Pitner, G. Giri, J. H. Koo, J. Park, K. Kim, H. Wang, R. Sinclair, H. S. Wong and Z. Bao, *Adv. Mater.*, 2015, **27**, 2656–2662.
13 X. Li, Y. Jung, K. Sakimoto, T.-H. Goh, M. A. Reed and A. D. Taylor, *Energy Environ. Sci.*, 2013, **6**, 879.
14 D. D. Tune, A. J. Blanch, C. J. Shearer, K. E. Moore, M. Pfohl, J. G. Shapter and B. S. Flavel, *ACS Appl. Mater. Interfaces*, 2015, **7**(46), 25857–25864.
15 D. Vennerberg and M. R. Kessler, *Carbon*, 2014, **80**, 433–439.
16 H. Shimoda, S. J. Oh, H. Z. Geng, R. J. Walker, X. B. Zhang, L. E. McNeil and O. Zhou, *Adv. Mater.*, 2002, **14**, 899–901.
17 M. Engel, J. P. Small, M. Steiner, M. Freitag, A. A. Green, M. C. Hersam and P. Avouris, *ACS Nano*, 2008, **2**, 2445–2452.
18 H. Ko and V. V. Tsukruk, *Nano Lett.*, 2006, **6**, 1443–1448.
19 Y. Joo, G. J. Brady, M. S. Arnold and P. Gopalan, *Langmuir*, 2014, **30**, 3460–3466.
20 B. S. Flavel, K. E. Moore, M. Pfohl, M. M. Kappes and F. Hennrich, *ACS Nano*, 2014, **8**, 1817–1826.
21 B. S. Flavel, M. M. Kappes, R. Krupke and F. Hennrich, *ACS Nano*, 2013, **7**, 3557–3564.
22 D. L. White and G. N. Taylor, *J. Appl. Phys.*, 1974, **45**, 4718–4723.
23 D. S. Hecht, A. M. Heintz, R. Lee, L. Hu, B. Moore, C. Cucksey and S. Risser, *Nanotechnology*, 2011, **22**, 169501.
24 N. Behabtu, C. C. Young, D. E. Tsentalovich, O. Kleinerman, X. Wang, A. W. K. Ma, E. A. Bengio, R. F. ter Waarbeek, J. J. de Jong, R. E. Hoogerwerf, S. B. Fairchild, J. B. Ferguson, B. Maruyama, J. Kono, Y. Talmon, Y. Cohen, M. J. Otto and M. Pasquali, *Science*, 2013, **339**, 182–186.
25 A. B. Reising, R. J. Moon and J. P. Youngblood, *J. Sci. Technol. Forest Products Processes*, 2012, **2**, 32–41.
26 J. T. Jenkins, *Annu. Rev. Fluid Mech.*, 1978, **10**, 197–219.
27 T. Börzsönyi, B. Szabó, G. Törös, S. Wegner, J. Török, E. Somfai, T. Bien and R. Stannarius, *Phys. Rev. Lett.*, 2012, **108**, 228302.
28 R. Zhang, Z. Ning, Y. Zhang, Q. Zheng, Q. Chen, H. Xie, Q. Zhang, W. Qian and F. Wei, *Nat. Nanotechnol.*, 2013, **8**, 912–916.

 